

MOVING LINEAR ARRAY TECHNIQUE: IMPROVED LATERAL RESOLUTION WITH DECREASED SCAN TIME TO FORM A 3D IMAGE

Zalman M. Benenson, Alexey B. Elizarov, Tatiana V. Yakovleva
 Scientific Council on Cybernetics, Russian Academy of Sciences,
 Vavilova st. 40, Moscow, 119991, Russia
 William D. O'Brien, Jr.

Bioacoustics Research Laboratory, Department of Electrical and Computer Engineering, University of Illinois,
 405 N. Mathews, Urbana, IL 61801 U.S.A

Abstract – The paper proposes a method to form 3D images with improved resolution and significantly decreased frame rates. The method is based on a linear phased array with a cylindrical lens that is moving in the direction perpendicular to the electronic scanning plane. The theory, the algorithms of the dynamic focusing in 3D space, the results of simulation and physical experiment results are given.

I. INTRODUCTION

The theoretical basics and experimental verification of a new method is proposed that forms 3D images with improved resolution and significantly decreased frame rate. Image formation data are acquired from a linear phased array as the array moves in the direction perpendicular to the electronic scanning plane. The decreased scanning time is achieved by alternating between two transmit signals from the array's elements. In this scheme the resolution improvement is obtained by a special signal processing strategy, the so-called virtual array, that results in an apparent aperture twice as large as the physical aperture. In the plane of the array movement, a modification of the spatial-temporal Fourier transform is applied to the received signals that are dynamically focused in the electronic scanning plane.

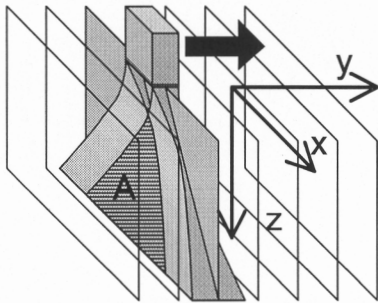


Fig. 1. Scheme of scanning.

II. THE SCANNING AND SIGNAL PROCESSING

Two wide-band ultrasonic pulses are transmitted sequentially in time from the two end elements of the linear phased array (Fig. 1). The echoes are received simultaneously by all the array elements. Then the array is incrementally shifted along the y-axis and the same transmit-receive procedure is repeated. After each transmit-receive procedure, the received data are preprocessed to accomplish dynamic focusing in the electronic scanning plane. After the array has been displaced by the required distance along the y-axis, the preprocessed signals are processed to form the 3D image.

A cylindrical lens with a fixed focal distance F is mounted on the array's surface. This provides for a constant lateral resolution within large depth intervals in the plane of movement along y-axis. This resolution is equal to the focal region's beamwidth.

III. THEORY

The spatial-temporal Fourier transform of the linear phased array's radiation pattern (with a convex cylindrical lens of focal distance F) is [1,2]:

$$u_{re}(\Omega_x, \Omega_y, \omega, z, \xi_n) = A(\Omega_y, \omega) A(\Omega_x) \times \exp(i\Omega_x \xi_n) \exp\left(iz \sqrt{\left(\frac{\omega}{c}\right)^2 - \Omega_x^2 - \Omega_y^2}\right) \quad (1)$$

where ξ_n is a coordinate of the array's elements, $A(\Omega_y, \omega)$ is the Fourier transform of the y-coordinate cylindrical lens function, $A(\Omega_x)$ is the Fourier transform of the array elements' x-coordinate radiation pattern, Ω_x and Ω_y are the spatial frequencies, and ω is the temporal frequency. For the

Fourier transform of the radiation pattern of the individual transmitting elements $u_{r,l}$, $u_{r,r}$, formula (1) can be used with ξ_n substituted with the coordinates of the left or right element, that is, respectively, $-\frac{L_x}{2}$ or $\frac{L_x}{2}$. The Fourier transform of the received signals, due to the left transmitting element, scattered by a point reflector with the coordinates (x_0, y_0, z_0) can be represented by:

$$\begin{aligned} \hat{S}_l(\Omega_x, \Omega_y, \omega, z, \xi_n) &= K_0 \int u_{re}(\Omega'_x, \Omega'_y, \omega, z, \xi_n) \times \\ &\times \exp(-i\Omega'_x x_0) \exp(-i\Omega'_y y_0) \times \\ &\times u_{r,l}\left(\Omega_x - \Omega'_x, \Omega_y - \Omega'_y, \omega, z, -\frac{L_x}{2}\right) \times \quad (2) \\ &\times \exp(-i(\Omega_x - \Omega'_x)x_0) \times \\ &\times \exp(-i(\Omega_y - \Omega'_y)y_0) d\Omega'_x d\Omega'_y \end{aligned}$$

The corresponding expression for the right transmitting element $\hat{S}_r(\bullet)$ is obtained by substituting $-\frac{L_x}{2}$ by $\frac{L_x}{2}$ in formula (2). We can approximate formula (2) as:

$$\begin{aligned} \hat{S}_l(\Omega_x, \Omega_y, \omega, z, \xi_n, x_0, y_0) &= B(\Omega_y, \omega) \times \\ &\times \exp\left(-i\frac{c(z-F)\Omega_y^2}{4\omega}\right) \exp(-i\Omega_y y_0) \times \\ &\times \int \exp(i\Omega'_x(\xi_n - x_0)) \times \\ &\times \exp\left(iz\sqrt{\left(\frac{\omega}{c}\right)^2 - \Omega_x'^2}\right) \times \quad (3) \\ &\times \exp\left(-i(\Omega_x - \Omega'_x)\left(-\frac{L_x}{2} - x_0\right)\right) \times \\ &\times \exp\left(iz\sqrt{\left(\frac{\omega}{c}\right)^2 - (\Omega_x - \Omega'_x)^2}\right) d\Omega'_x \end{aligned}$$

where $B(\Omega_y, \omega)$ determines the resolution along the y-axis. In order to obtain an expression for \hat{S}_r , substitute $-\frac{L_x}{2}$ by $\frac{L_x}{2}$ in formula (3).

The inverse Fourier transform by Ω_x of formula (3) is the following formula:

$$\begin{aligned} S_l(\Omega_y, \omega, z, x_0, y_0) &= \gamma_0 B(\Omega_y, \omega) \times \\ &\times \exp\left(-i\frac{c(z-F)\Omega_y^2}{4\omega}\right) \exp(-i\Omega_y y_0) \times \\ &\times \frac{1}{\sqrt{z^2 + x_0^2}} \exp\left(i\frac{\omega}{c}\left(\sqrt{r_0^2 + \xi_n^2} - 2\xi_n x_0 + \right. \quad (4) \right. \\ &\left. \left. + i\sqrt{r_0^2 + \left(\frac{L_x}{2}\right)^2} - 2\left(-\frac{L_x}{2}\right)x_0\right)\right) \end{aligned}$$

where $r_0 = \sqrt{z^2 + x_0^2}$, and γ_0 is the reflection coefficient of the point reflector. An expression for S_r is obtained by substituting $-\frac{L_x}{2}$ by $\frac{L_x}{2}$ in formula (4).

It is easy to see that for the conditions $|\xi_n| < r_0$ and $\frac{L_x}{2} < r_0$, formula (4) for S_l and the corresponding formula for S_r determine the approximate expressions for the signals received by the linear phased array with the elements' coordinates $\hat{\xi}_n = \xi_n - \frac{L_x}{2}$ and, respectively, $\hat{\xi}_n = \xi_n + \frac{L_x}{2}$, where $\hat{n} = -N, \dots, 0, \dots, N$ and N is the number of elements of the linear phased array. We call such an array a virtual array. Its length is two times larger than the actual array length.

To focus in the array's plane (the x-z plane), the received signals are appropriately summed for all the elements of the virtual array. An apodization function is applied, as is compensation of the differences in the signals' time delays between array elements and various points of the scattering medium. The time delays are calculated as:

$$\begin{aligned} \delta_{\hat{n}} &= -\frac{1}{c}\left(\sqrt{r_0^2 + \xi_n^2} - 2\xi_n x_0 + \right. \quad (5) \\ &\left. + \sqrt{r_0^2 + \left(\frac{L_x}{2}\right)^2} + 2\frac{L_x}{2}x_0 - 2z\right) \end{aligned}$$

for $\hat{n} = -N, \dots, 0,$

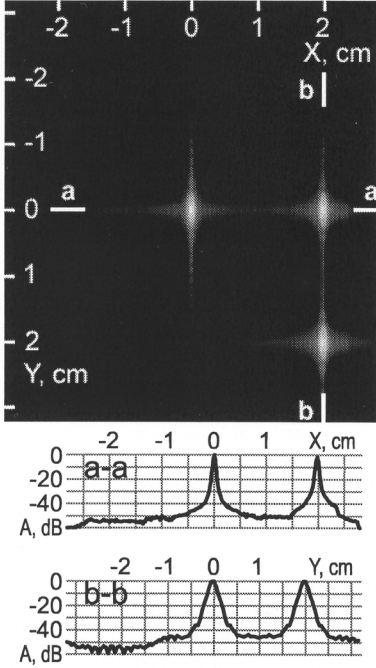


Fig. 2. Simulated image. Dynamic range 60 dB.

$$\delta_{\hat{n}} = -\frac{1}{c} \left(\sqrt{r_0^2 + \xi_n^2 - 2\xi_n x_0} + \sqrt{r_0^2 + \left(\frac{L_x}{2}\right)^2 - 2\frac{L_x}{2}x_0 - 2z} \right)$$

for $\hat{n} = 1, \dots, N$.

The main components of the signal processing algorithm consist in the following:

- The three-dimensional array of echo signals for every pair of transmitted ultrasound pulses are acquired. This takes into account the coordinates of receiving elements and the position of the moving phased array.

- Focusing in the x-z plane of electronic scanning as described above.

- The Fourier transform of received signals by time and by y-coordinate of the array's position. The 2D Fourier transform for the set of scattering points with coordinates (x_n, y_n, z) can be expressed as:

$$S_0(x, \Omega_y, \omega, z) = \sum_n \gamma_n B(\Omega_y, \omega) \exp(i2\omega z) \times \exp\left(-i\frac{c(z-F)\Omega_y^2}{4\omega}\right) \exp(-i\Omega_y y_n) \times L(x - x_n, x_n, z) \quad (6)$$

where γ_n is the reflection coefficient of corresponding point reflectors, and $L(x - x_n, x_n, z)$ is the focused radiation pattern in the x-z plane.

- Then the function (6) is corrected to take into account the focusing in the y-z plane. The corresponding algorithm is described in [2,3].

- Implementation of the inverse Fourier transform by the frequencies Ω_y and ω of the function obtained in the previous step.

IV. RESULTS

Fig. 2 illustrates the results of the mathematical simulation. Three point reflectors in the x-y plane at $z=4.5$ cm were used for this simulation. The two graphs below the image in Fig. 2 are the signal magnitudes in x and y directions. The center frequency was 3.5 MHz, the length of the array was 2.8 cm and the width of the array (of the lens) was 0.6 cm. The focal distance F of the lens was 3.0 cm. The -10-dB lateral resolution in the x-z scanning plane was 0.07 cm, and exceeds 2 times the Rayleigh limit. The -10-dB lateral resolution in the y-z plane was 0.24 cm.

To experimentally verify the proposed technique a transmit-receive system was fabricated, and used with a micropositioning system to precisely control the array's position. The array was positioned and moved in a temperature-controlled water bath. The array scanned a 3D wire phantom that was also in the water bath. The phantom was shaped as Cyrillic letters "HCK PAH" that were made of twice twisted 0.15-mm-diameter cuprum wires. Each letter was oriented in the x-y plane and positioned at different depths z .

Fig. 3 shows 2D images in the x-z plane (panel 1) and the y-z plane (panel 2), and illustrates the depth positions of each of the 6 letters. The 2D image orientation of these two panels is typical of modern diagnostic ultrasound imaging systems. It is not possible to recognize the letters by means of these cross-sections. The 2D images in the y-z plane (panels 3-8) at various depths z show the 6 letters that are clearly recognized.

The proposed technique was additionally verified by using experimentally-derived echo signals that were propagated in a tissue-like medium. The digital database of a phased array was obtained from the Biomedical Ultrasonics Laboratory, University of Michigan (<http://bul.eecs.umich.edu>). The primary data were transformed in such a way that allowed forming the signals transmitted by the right and left

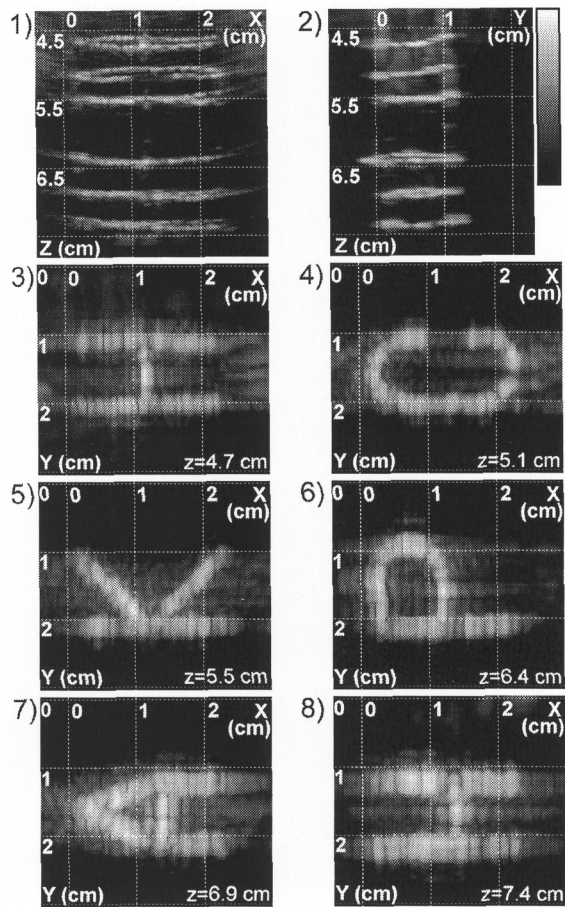


Fig. 3. Letter image. Dynamic range 40 dB.

elements of the array and then received by all of the array elements. The array length was 2.8 cm with a frequency of 3.5 MHz. Fig. 4 illustrates the processed 2D image of the phantom with point reflectors. After image formation by the virtual array method, the sizes of the reflectors at the level of -10 dB ranged from 0.10 cm at $z=4.5$ cm to 0.17 cm at $z=10.5$ cm which is close to the theoretical estimation $\frac{\lambda z}{2a}$, where λ is the wavelength and $2a$ is the length of the array's aperture.

V. CONCLUSION

The results demonstrate that it is possible to achieve fast frame rate for 3D imaging in an azimuth sector of 60° . The transducer's movement length was 3 cm, the maximum depth was 15 cm and the frequency was 3.5 MHz. The frame rate was around 0.01 sec. The lateral resolution in the x-z scanning

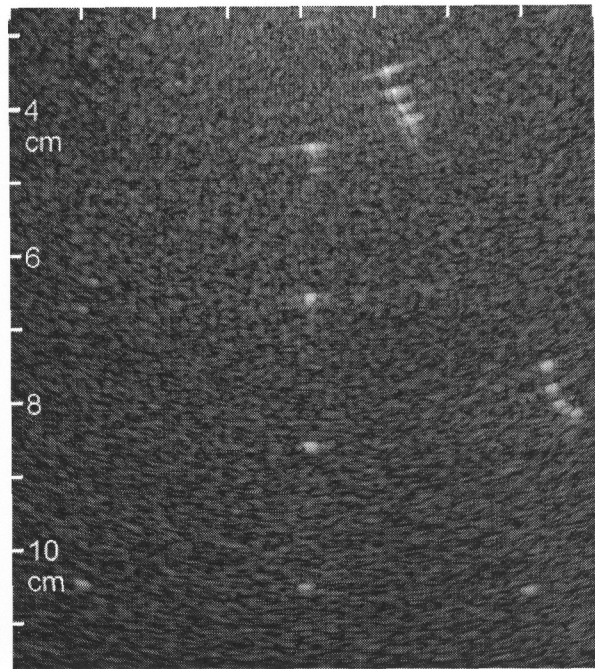


Fig. 4. Phantom image. Dynamic range 60 dB.

plane was 2 times better than the Rayleigh limit and was independent of depth.

VI. ACKNOWLEDGEMENTS

This work has been partly supported by CRDF (USA) RP2-2104 and by the RFFI (Russia) N02-01-01087.

VII. REFERENCES

- [1] J. W. Goodman. "Introduction to Fourier Optics", McCrow Hill Book Company, 1968.
- [2] Z. M. Benenson, A. B. Elizarov, T. V. Yakovleva, W. D. O'Brien, Jr., "Approach to 3D Ultrasound High Resolution Imaging Based upon Fourier Transform", IEEE Trans. Ultrason., Ferroelect., Freq. Contr., in press.
- [3] Z. M. Benenson, A. B. Elizarov, T. V. Yakovleva, W. D. O'Brien, Jr., "Depth-Independent Narrow Beamwidth 3D Ultrasonic Image Formation Technique", in this Proceedings.